

Modifiers of solid RNP granules control normal RNP dynamics and mRNA activity in early development

Arnaud Hubstenberger,^{1,3} Cristiana Cameron,¹ Scott L. Noble,^{1,2} Sean Keenan,¹ and Thomas C. Evans¹

¹Department of Cell and Developmental Biology and ²Graduate Program in Molecular Biology, School of Medicine, University of Colorado Anschutz Medical Campus, Aurora, CO 80045

³Pierre-and-Marie-Curie University, University Paris 06, 75005 Paris, France

Ribonucleoproteins (RNPs) often coassemble into supramolecular bodies with regulated dynamics. The factors controlling RNP bodies and connections to RNA regulation are unclear. During *Caenorhabditis elegans* oogenesis, cytoplasmic RNPs can transition among diffuse, liquid, and solid states linked to mRNA regulation. Loss of CGH-1/Ddx6 RNA helicase generates solid granules that are sensitive to mRNA regulators. Here, we identified 66 modifiers of RNP solids induced by *cgh-1* mutation. A majority of genes promote or suppress normal RNP body assembly, dynamics, or metabolism. Surprisingly, polyadenylation factors promote RNP coassembly in vivo, suggesting new functions of poly(A) tail regulation in RNP dynamics. Many genes carry polyglutamine (polyQ) motifs or modulate polyQ aggregation, indicating possible connections with neurodegenerative disorders induced by CAG/polyQ expansion. Several RNP body regulators repress translation of mRNA subsets, suggesting that mRNAs are repressed by multiple mechanisms. Collectively, these findings suggest new pathways of RNP modification that control large-scale coassembly and mRNA activity during development.

Introduction

Large coassemblies of nucleic acids and proteins are a common but poorly understood feature of gene expression pathways. In the nucleus, chromatin and RNPs condense into multiple supramolecular domains, bodies, and “speckles” (Mao et al., 2011; Rinn and Guttman, 2014). In the cytoplasm, a variety of RNP granules can form, including processing bodies (PBs), stress granules, and diverse RNP bodies in nervous system, germ cells, and embryos (Decker and Parker, 2012; Buchan, 2014; Schisa, 2014). The functions and control of supramolecular RNP bodies remain elusive.

RNP granules are dynamic and tightly regulated in vivo. Remarkably, biophysical studies showed that three different native RNP bodies behave like liquid droplets in living cells (Brangwynne et al., 2009, 2011; Hubstenberger et al., 2013). Given the dynamic nature of other granules, liquid-like states are likely common (Hyman et al., 2014). In *Caenorhabditis elegans*, fluidity and sorting within RNP bodies are precisely controlled by developmental cues, and similar controls are likely widespread (Weber and Brangwynne, 2012; Hubstenberger et al., 2013; Hyman et al., 2014). RNPs can also polymerize into solid structures. Defects or polyglutamine (polyQ) expansions in some RNA regulators can induce large solid aggregates, which are common in central nervous system (CNS) diseases (King et al., 2012; Ramaswami et al.,

2013). In the normal CNS, prion-like (solid) RNP polymers may contribute to long-term potentiation (Si et al., 2010; Heinrich and Lindquist, 2011). Collectively, these findings suggest that RNP condensations are carefully regulated, influencing RNP dynamics and fate.

Factors that control RNP dynamics in vivo remain to be elucidated. RNP condensation involves multivalent interactions among proteins and RNAs. In vitro, large-scale coalescence can be driven by stereospecific interactions or by divergent disordered protein domains (Han et al., 2012; Kato et al., 2012; Li et al., 2012; Malinowska et al., 2013). Presumably, the control of RNP coassembly in living systems involves pathways that modulate such interactions. The nature of these pathways is largely unknown.

Development within the *C. elegans* germline reveals the remarkable precision and complexity of RNP coassembly control. During adult oogenesis, several different cytoplasmic RNP bodies undergo regulated transformations, in concert with specific patterns of mRNA regulation (Fig. 1; Schisa et al., 2001; Boag et al., 2005, 2008; Gallo et al., 2008; Jud et al., 2008; Noble et al., 2008; Schisa, 2014). All share some components with PBs and stress granules of other cells and with each other, but each has unique composition and dynamics. Large germline RNP bodies, called germline

Correspondence to Thomas C. Evans: tom.evans@ucdenver.edu

Abbreviations used in this paper: CNS, central nervous system; grPB, germline mRNP processing body; IDR, intrinsically disordered region; IF, immunofluorescence; mRNP, messenger RNP; PB, processing body; polyQ, polyglutamine; RAP, RNA-associated protein; RBP, RNA-binding protein.

© 2015 Hubstenberger et al. This article is distributed under the terms of an Attribution-Noncommercial-Share Alike-No Mirror Sites license for the first six months after the publication date (see <http://www.rupress.org/terms>). After six months it is available under a Creative Commons License (Attribution-Noncommercial-Share Alike 3.0 Unported license, as described at <http://creativecommons.org/licenses/by-nc-sa/3.0/>).

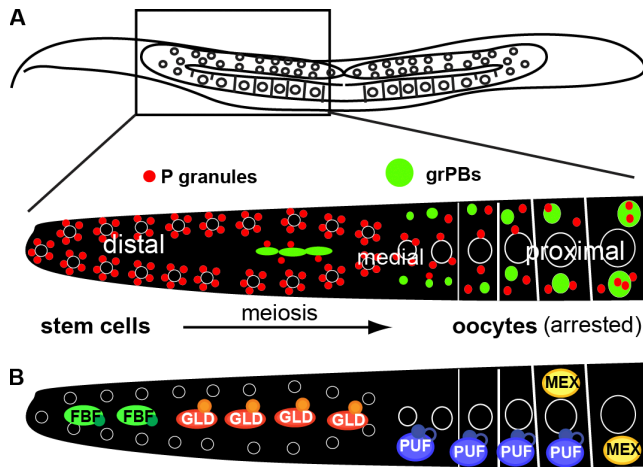


Figure 1. *C. elegans* germline development controls RNP bodies and mRNA regulators. One arm of the gonad (top diagram) is depicted unfolded (A and B). Stem cells enter meiotic prophase in distal gonad, undergo prophase transitions in medial gonad, and differentiate into oocytes in proximal gonad. (A) Different RNP bodies undergo transformations during oogenesis. (B) RBP translation repressors are expressed with spatio-temporal specificity linked to oogenesis stages.

messenger RNP (mRNP) processing bodies (grPBs), form in arrested oocyte cytoplasm, where they recruit repressed mRNAs, RNA-binding protein (RBP) repressors, and specific PB proteins (Jud et al., 2008; Noble et al., 2008). Distinct germ granules (P granules) associate with nuclei in early stage germ cells, dissociate into the cytoplasm, and eventually merge with grPBs in differentiated oocytes (Jud et al., 2008; Noble et al., 2008; Updike and Strome, 2010; Hubstenberger et al., 2013). RNP transformations occur within a precise spatiotemporal program of germ cell development (Fig. 1 A). Driving this program are specific RBP repressors that generate specific patterns of mRNA translation (Fig. 1 B; Nusch and Eckmann, 2013). Therefore, diverse RNP assemblies and mRNA control systems are precisely regulated during oogenesis, suggesting important interrelationships of these processes.

Previous work suggested that mRNP modulation controls RNP body dynamics in the *C. elegans* germline. Translational repressors stimulate RNP condensation into large semiliquid grPBs (Hubstenberger et al., 2013). RNPs are modulated directly or indirectly by the CGH-1/Ddx6 RNA helicase to prevent nondynamic solidification; loss of *cgh-1* transforms some grPB factors from dynamic states into solid square granules (Audhya et al., 2005; Boag et al., 2005; Noble et al., 2008; Hubstenberger et al., 2013). Some RBP repressors promote *cgh-1(lf)* solid sheet formation, normal semiliquid grPB condensation, and repression of mRNAs (Noble et al., 2008; Hubstenberger et al., 2012, 2013; Nusch and Eckmann, 2013). To further understand this pathway, we sought in this study to identify new regulators of helicase-modulated RNP polymerization and comprehensively test their roles in grPB and mRNA regulation. Several additional RNA control factors were found that influence grPBs in distinct ways and promote several mRNA repression systems. Collectively, these genes suggest that multiple pathways of RNA regulation from the nucleus to the cytoplasm collaborate to modulate large-scale RNP co-assembly and mRNA translation.

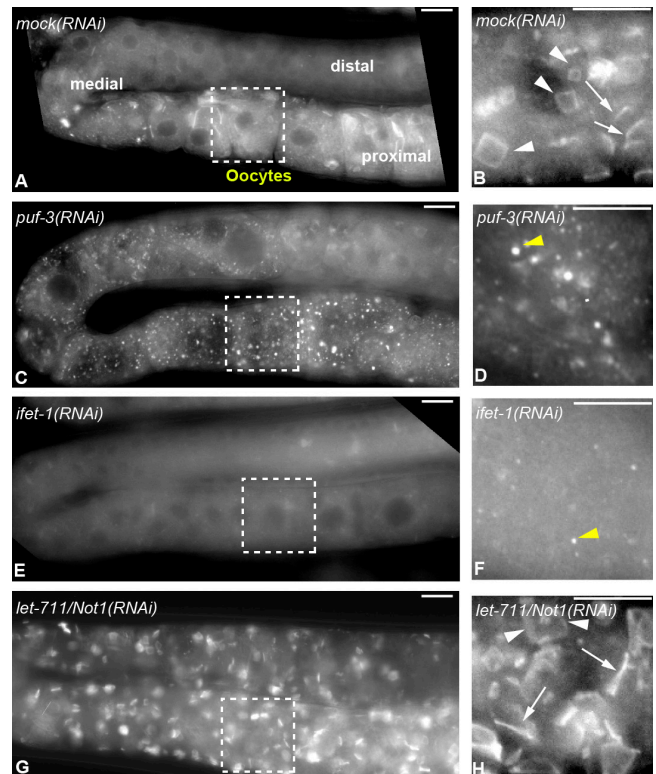


Figure 2. RNAi screen reveals different impacts on solid granules. At left, live *cgh-1(tm691)* epifluorescence images show GFP:CAR-1 throughout gonads (labeled in A; see Fig. 1). At right, enlarged views show oocytes from different individuals (equivalent of dashed boxes at left). Bars, 10 μ m. (A) After control RNAi (*mock*), solid square granules and diffuse GFP:CAR-1 were seen throughout. (B) Solid granules viewed from top/bottom revealed square shapes (white arrowheads), whereas lateral views revealed thin sheet sides (white arrows). After *puf-3* (C-D) or *ifet-1* (E and F) RNAi, solid granules were disrupted into small puncta (yellow arrowheads) and increased diffuse GFP:CAR-1. After *let-711/Not1* RNAi (G and H), square sheet numbers increased.

Results

Genes that modify aberrant RNP solids are enriched for RNA control factors

To identify new regulators of cytoplasmic RNP particles in *C. elegans* gonads, we conducted a primary RNAi screen for modifiers of solid GFP:CAR-1 sheets that form in the *cgh-1(tm691ts)* mutant (Figs. 2 and 3). CAR-1 is a homologue of human Lsm14, is a core constituent of *cgh-1(lf)* solid granules and normal grPB droplets, and promotes both grPB assembly and mRNA repression (Audhya et al., 2005; Boag et al., 2005; Noble et al., 2008). To target adult oogenesis and bypass early germline development, RNAi and temperature upshift were induced for limited duration late in development. To facilitate multiple secondary assays, we screened a subset of 999 genes likely enriched for germline RNP regulators (Table S1): (a) 925 genes with oogenesis-enhanced expression (Reinke et al., 2004) and (b) 74 additional genes that confer embryo osmotic resistance, a function of some known RNP granule modulators (*puf-5*, *car-1*, and *cgh-1*; Sönnichsen et al., 2005; Lublin and Evans, 2007; Noble et al., 2008).

RNAi of 66 genes altered the size, morphology, or abundance of square sheet granules in *cgh-1(tm691ts)* gonads while maintaining GFP:CAR-1 expression, with the exception

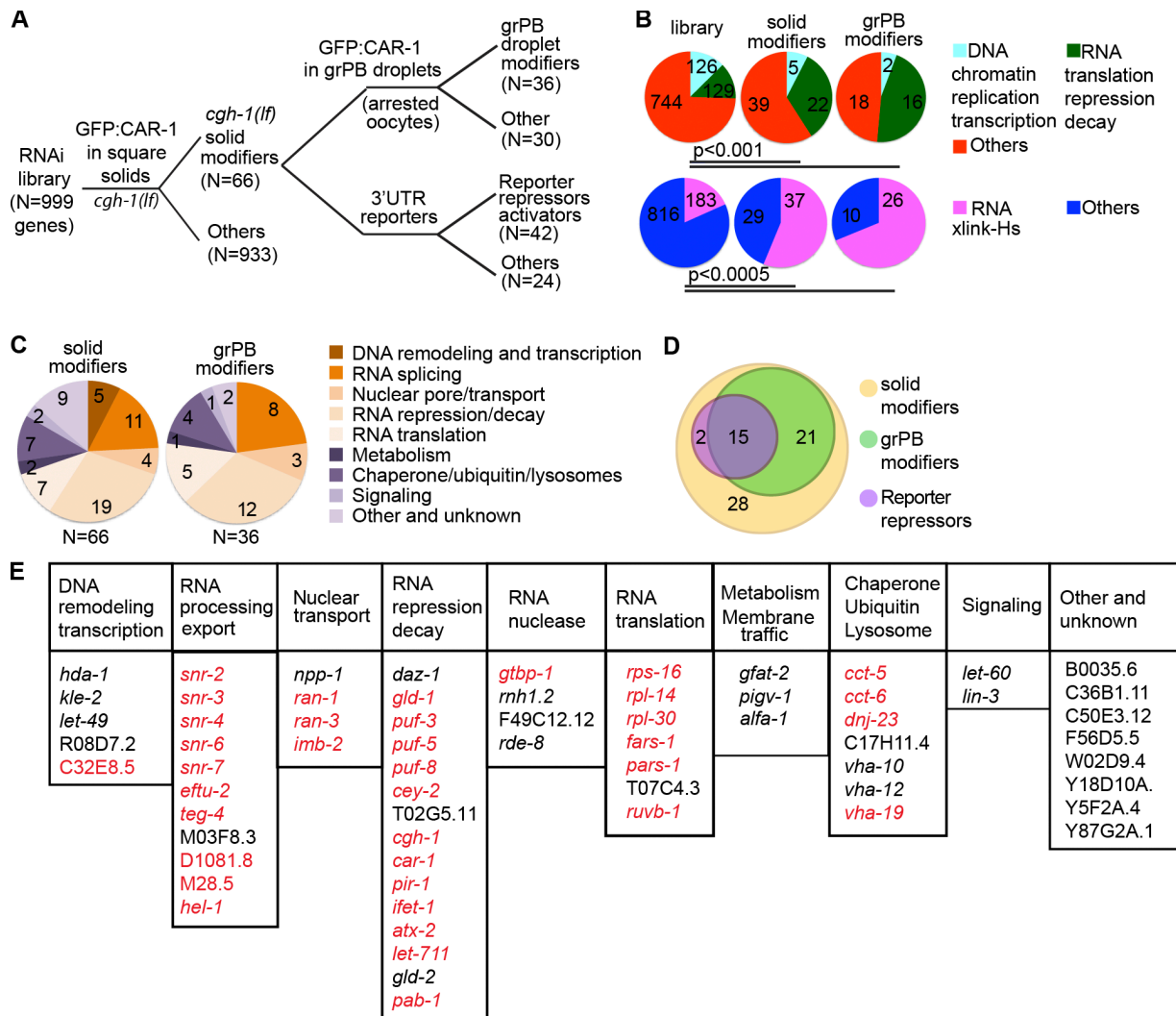


Figure 3. Overview and summary of RNAi screens. (A) Schematic overview of screen strategy. Modifiers of solid granules in *cgh-1(tn691)* were identified from RNAi sublibrary (Fig. 2 and Table S2). Screen positives were tested for effects on semiliquid grPBs (Fig. 4 and Table S3) and regulation of 3' UTR reporters (Fig. 7). (B) Upper row shows enrichment of COG RNA control terms compared with DNA control for the library, *cgh-1(tn691)* solid modifiers, and grPB modifiers. Lower row shows significant enrichment for homologues of human proteins that cross-link to RNAs (Castello et al., 2012). (C) Direct homology analyses revealed most genes promote RNA controls. (D) Overlap of genes from screens in (A). (E) Solid modifiers are listed (categories as in C); genes in red are homologues of human RNA-linked proteins (as in B).

of *car-1*, which eliminated GFP:CAR-1 fluorescence (Fig. 2 and Table S2). A majority of RNAi depletions induced smaller puncta and/or more diffuse GFP, either throughout the gonad or only in proximal regions (Fig. 2, compare C–F with A and B; and Fig. S1, K and L). These phenotypes suggest suppressed solid granule formation or maintenance. Consistent with this idea, *puf-5* promotes RNP coassembly and was independently found here as a solid granule suppressor (Hubstenberger et al., 2013; Table S2). Some genes caused increased granule number, suggestive of enhanced RNP solid formation (Fig. 2, G and H; and Table S2). In support of this, *cgh-1* itself was identified in this group. Variations were seen within these two groups, and some knockdowns gave complex phenotypes (Table S2). Some defects could impact granule (or component) synthesis, turnover, or indirect pleiotropic pathways. Regardless, these 66 genes suggest functions that promote, suppress, or modulate RNP solid particles formed in a pathological (*cgh-1* mutant) state.

Several positives were known regulators of mRNPs, including the mRNA-specific RBPs PUF-5, PUF-3, and GLD-1

(Lublin and Evans, 2007; Hubstenberger et al., 2012; Nousch and Eckmann, 2013). To test screen specificity further, we compared NCBI COG terms in the library and screen positives (Tatusov et al., 2003). We found substantial enrichment of “RNA control” genes ($P < 0.001$) and reduced representation of other gene classes, such as “DNA control” genes (Fig. 3 B). To analyze gene classes in more detail, we further annotated genes by direct homology inspection, which revealed that 56% of positives (37/66) have predicted activities in RNA binding, translation, splicing, translational regulation, or decay (Fig. 3, C–E). Collectively therefore, modifiers of *cgh-1(lf)* solid granules are strongly enriched for functions in RNP control.

Several genes fell into categories not clearly tied to RNA biology, most of which have human homologues (Fig. 3 E and Table S2). Although these genes could act indirectly, several findings suggest possible novel functions in RNP control. Two Ras signaling genes (*let-60/Ras* and *lin-3/EGF*) promoted solid granule formation, which is supported by direct or posttranscriptional control of RBP-mediated mRNA repression by the Ras pathway in

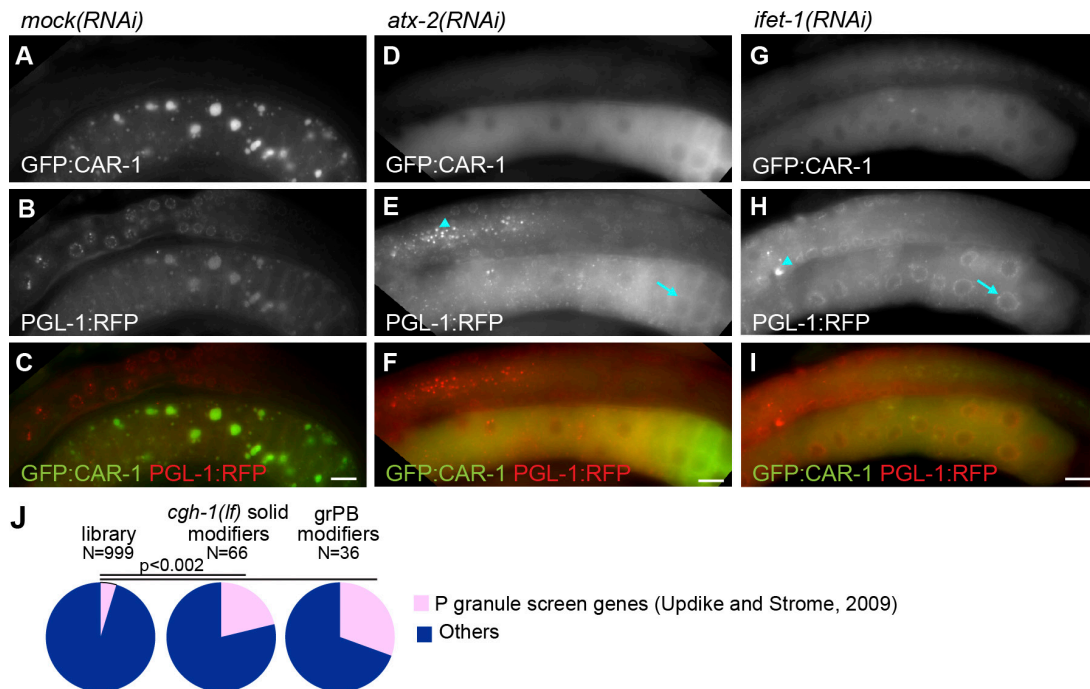


Figure 4. Solid modifiers promote semiliquid grPB coalescence. Shown are gonads of live animals expressing GFP:CAR-1 and PGL-1:RFP after physiological oogenesis arrest. (A–C) In control gonads, GFP:CAR-1 (A) condenses into semiliquid grPBs, whereas PGL-1:RFP (B) forms distinct P granules that transition from nucleus-attached, to cytoplasm, and to separate grPB subdomains as oocytes differentiate. (D–I) After *atx-2(RNAi)* and *ifet-1(RNAi)*, GFP:CAR-1 (D and G) coassembly was disrupted. PGL:RFP particles (E and H) accumulated in medial core (arrowheads) and on nuclei in proximal oocytes (arrows). (J) Most solid modifiers were not identified in previous P granule modifier screen (Updike and Strome, 2009), whereas a subset common to both datasets was enriched.

oogenesis (Arur et al., 2011; Hubstenberger et al., 2012). Intriguingly, screen positives were threefold enriched for homologues of human proteins that can be UV cross-linked in vivo to polyadenylated RNAs in HeLa cells (Fig. 3, B and E; Castello et al., 2012). Some of these were unexpected, including the TRiC chaperonin (*cct-6/CCT6*), the chaperone DNAJC9 (*dnj-23*), and a subunit of vacuolar proton-translocating ATPase (*vha-19/ATP6A1*). Additional subunits of these protein complexes were also identified (Fig. 3 E). Thus, our *C. elegans* screen links RNP control functions to unpredicted human mRNA-binding proteins that control protein folding (chaperones) and membrane trafficking (*vha* genes). Two additional genes support roles of membrane vesicle dynamics (*alfa-1* and *pigv-1*; Farg et al., 2014; Budirahardja et al., 2015). Interestingly, *alfa-1* is a homologue of human *c9orf72*, which is the most common target of polyQ expansions in some CNS diseases that are linked to RNP aggregation (Mizielinska and Isaacs, 2014). Therefore, the RNP solidification modifier screen revealed not only predicted RNP regulators but also genes that could play novel roles in RNP dynamics. Subsequent analyses of grPB dynamics and mRNA control support this view for at least some genes.

Modifiers of aberrant solid granules control normal RNP bodies

To determine if RNP solid modifiers influence normal RNP dynamics, we depleted all positive genes in females that form large semiliquid grPBs marked with GFP:CAR-1 and P granules marked with PGL-1:RFP. Among the 66 primary screen genes, RNAi of 36 led to defects in condensation, size, or morphology of grPB droplets in arrested oocytes of live animals (Fig. 3, B–D; Fig. 4; and Table S3). A majority (20/36) reduced grPB size and/or caused GFP:CAR-1 dissolution (Fig. 4, A–I;

and Table S3). These “class I” phenotypes suggest genes that normally promote or maintain grPB condensation. In support of this, at least four class I gene depletions (*atx-2*, *gld-2*, *car-1*, and *puf-5*) also inhibited condensation of other grPB components (Fig. S1; Noble et al., 2008; Hubstenberger et al., 2013). Furthermore, all class I gene depletions also suppressed solid granules in *cgh-1(tm691)*, consistent with roles in promoting large-scale multimerization (Fig. 2, C–F; and Table S2). Among grPB modulators, most known mRNA-specific RBP repressors (e.g., PUF-3, PUF-5, GLD-1) and predicted mRNA-associated proteins (e.g., DAZ-1, ATX-2, IFET-1, CAR-1) were class I genes (Table S3). By contrast, several gene knockdowns (14/35) altered grPBs into square sheets or into square-edged, elongated, or enlarged granules (Fig. 5, B and H; and Table S3). These “class II” phenotypes are diverse but generally are suggestive of genes that normally suppress grPB condensation, growth, or solidification as seen for CGH-1 (Hubstenberger et al., 2013). Consistent with this idea, 12/14 class II genes induced square sheets in this assay or enhanced solid sheet formation in *cgh-1(tm691)* gonads (Fig. 2, G and H; and Tables S2 and S3). Class II genes were enriched for mRNA splicing and export factors. Some phenotypes in either class could result indirectly from oogenesis defects. For class I gene knockdowns, a majority disrupted grPBs in gonads that accumulated differentiated oocytes (oocyte “stacking”) without obvious oocyte maturation or ovulation increases, suggesting grPB defects are not likely because of defective oocyte arrest in these cases (Table S3). However, because some RNAi treatments did produce oocyte phenotypes and meiotic arrest was not quantified, indirect effects cannot be ruled out (Table S3). In addition, some phenotypes could reflect altered levels of

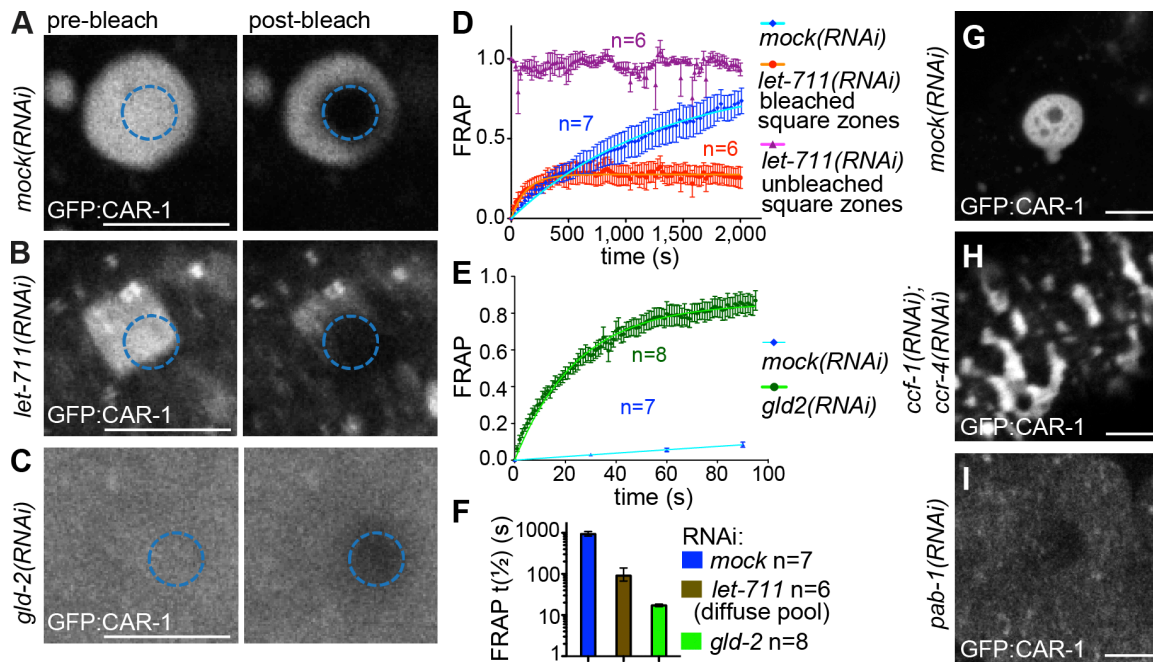


Figure 5. **Poly(A) tail regulators control RNP granule dynamics.** (A–D) Confocal sections of GFP:CAR-1 in arrested oocytes before and after photobleaching of a 2- μ m zone. GFP:CAR-1 labeled grPBs after control (*mock*) RNAi (A) and square sheets after *let-711/Not1* RNAi (B) and was diffuse after *gld-2* RNAi (C). (D) FRAP rates of photobleached GFP:CAR-1 zones showed total recovery in control grPBs (blue) but ~25% recovery in *let-711/Not1* RNAi square sheets (red), revealing a large immobile pool. GFP:CAR-1 remained in unbleached square sheet zones (purple), supporting a solid state. (E and F) GFP:CAR-1 FRAP half-times were ~100 times faster in *gld-2* RNAi oocytes than in control grPBs and ~10 times faster than diffuse cytosolic pool in *let-711/Not1* RNAi gonads. (G–I). GFP:CAR-1 formed elongated granules after double RNAi of CCF-1 and CCR-4 deadenylases (H) but dispersed after PAB-1 loss (I). Bars, 10 μ m.

specific factors, or other features of grPB metabolism. Another group of solid modifiers (30/66) did not obviously alter grPBs in normal arrested gonads (Table S3); solid granules could be more sensitive than grPBs to partial gene product loss, or some genes may specifically influence these aberrant polymers. Regardless, many solid modifiers control formation or dynamics of normal liquid-like grPBs during oogenesis. Some modifiers promote grPB condensation (class I genes), whereas others suppress condensation or solid granule formation (most class II genes).

Several genes also influenced P granules in arrested gonads. Some RNAi depletions disrupted PGL-1:RFP granules, whereas others enhanced P granule size, number, or retention on oocyte nuclei (Fig. 4, E and H; and Table S3). P granule effects of some of these genes were also seen in activated gonads previously (Updike and Strome, 2009; Sengupta et al., 2013). Therefore, these factors function in both grPB and P granule control, either through independent effects or because of links between P granule and grPB dynamics. To further explore these relationships, we compared our dataset to a previous genome-wide screen for P granule regulators in activated gonads and embryos (Updike and Strome, 2009). A subset of solid (14/66) and grPB (11/36) modifiers is shared with this P granule dataset (Fig. 4 J). However, most solid (52/66) and grPB (25/36) modifiers found here were not identified in the P granule screen (Fig. 4 J and Tables S2 and S3). In addition, most P granule modifiers that were in our sublibrary (33/47) were not identified as solid modifiers (Table S2). Although some differences likely reflect false negatives or experimental biases, some protein categories are unique to each dataset (e.g., polyadenylation activators and Ras pathway genes in solid granule screen; replication and cell cycle genes in P granule

screen; Table S2). Collectively, these findings support both specific commonalities and differences in control of these two distinct RNP granule types.

Poly(A) tail regulators control RNP coassembly dynamics

Three grPB modulators control mRNA poly(A) tail lengths or function in *C. elegans* and other species (*let-711/Not1*, *gld-2*, and *pab-1*; Nousch et al., 2013, 2014; Jalkanen et al., 2014). Longer poly(A) tails are generally associated with translation enhancement, and translationally active mRNAs are excluded from grPBs whereas translation repressors promote grPB formation (Noble et al., 2008; Hubstenberger et al., 2013; Jalkanen et al., 2014). Thus, a simple prediction is that poly(A) tail activators might inhibit condensation whereas poly(A) shortening factors might promote grPB formation like RBP repressors. Surprisingly, however, loss of the deadenylation factor LET-711/Not1 induced square sheet granules and diffuse GFP:CAR-1, similar to CGH-1 loss (Fig. 5, A and B; Hubstenberger et al., 2013). Square granules suggest CAR-1 solidification. To test this, we performed FRAP of GFP:CAR-1 in *let-711* RNAi square granules (Fig. 5, A, B, and D). Indeed, photobleached granule regions failed to recover most GFP:CAR-1, strongly supporting a solid particle core with minimal exchange (Fig. 5 D). Thus, deadenylation or other LET-711/Not1 functions inhibit RNP solidification. If deadenylation inhibits polymerization, then poly(A) addition may instead promote coassembly and slow dynamics. In support of this, RNAi of the GLD-2 poly(A) polymerase induced GFP:CAR-1 dissolution in many gonads, and mobility was increased almost 100-fold over controls and 10-fold over the diffuse soluble pool in *let-711* RNAi gonads (Fig. 5, C, E, and F). Furthermore,

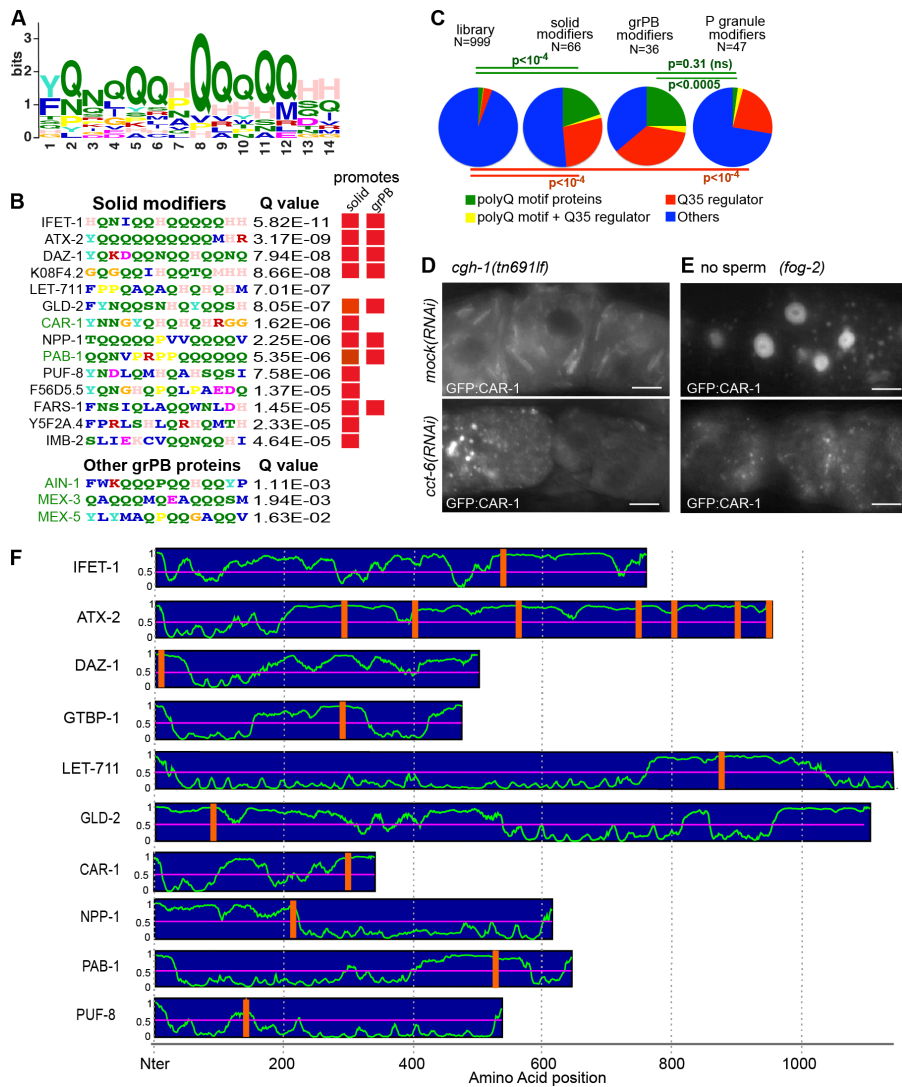


Figure 6. PolyQ domain regulation is linked to large-scale RNP coassembly. (A) PolyQ consensus motif was found among solid granule modulators. (B) Specific motifs among solid and grPB modulators (top) and three other known grPB proteins (bottom; known grPB proteins in green). Proteins that promote grPB or solid granule formation are marked (red boxes). (C) Poly Q motif proteins (green) were enriched among solid and grPB modifiers, but not among P granule modifiers from Updike and Strome (2009) that were in library (ns, not significant). Modifiers of Q35 aggregation that lack (red) or carry (yellow) polyQ motifs were enriched in all datasets. (D and E) CCT-6 (D and E) and CCT-5 (Tables S3 and S4) of the TriC chaperonin complex were required for solid granule (D) and large grPB formation (E). (F) All polyQ motifs reside in predicted IDRs.

PAB-1 depletion similarly caused strong grPB dissolution (Fig. 5 I). Thus, both a poly(A) polymerase (GLD-2) and a poly(A) tail effector (PAB-1) are required for condensation. By contrast, simultaneous depletion of two deadenylases, CCF-1 and CCR-4, induced elongated GFP:CAR-1 coassemblies, unlike spherical shapes expected of liquid-like droplets (Fig. 5 H). Other studies showed that LET-711/Not1, CCF-1, CCR-4, and GLD-2 are the major regulators of mRNA poly(A) tail lengths in *C. elegans*, at least in the germline (Nousch et al., 2013, 2014). Therefore, factors that stimulate poly(A) tail function (GLD-2 and PAB-1) slow RNP dynamics and promote grPB formation, whereas deadenylation factors prevent solidification (LET-711/Not1) or abnormal growth (CCF-1 and CCR-4). These functions contrast with simple predictions from proposed roles of poly(A) tails in translation.

PolyQ-disordered domain proteins and polyQ aggregation regulators control grPB coassembly

RNP bodies form by collective coassembly of multiple components. Thus, grPB modifiers might share features that modulate these interactions. To test this idea, we searched for common domains among *cgh-1(tm691)* solid modifiers. MEME and FIMO analyses identified a glutamine-rich (polyQ) motif that

was enriched ninefold ($P < 10^{-7}$) among solid modifiers compared with the total library (Fig. 6, A–C). By contrast, this polyQ motif was not enriched among P granule modulators present in our sublibrary ($P = 0.31$), suggesting specific connections to grPB and solid granule regulation (Fig. 6 C and Table S2; Updike and Strome, 2009). Most polyQ domain factors promoted condensation (Fig. 6 B and Table S3). In addition, five known grPB proteins carry related polyQ motifs, two of which were found in these screens (CAR-1 and PAB-1; Fig. 6 B). These findings are consistent with the idea that collective interactions among numerous polyQ motifs may specifically modulate grPB condensation. In vitro studies showed that intrinsically disordered regions (IDRs) with divergent sequences can also drive large-scale coassembly (Kato et al., 2012). Interestingly, we found that all polyQ motifs reside within larger predicted IDRs (Fig. 6 F and not depicted). Thus, polyQ motifs embedded in divergent disordered regions could control multivalent interactions in semiliquid grPBs.

If polyQ interactions contribute to grPB coassembly, genes that modulate such interactions might also be granule modulators. We found 14 genes that were independently identified as modifiers of pathological aggregation of a synthetic polyglutamine peptide (Q35) in somatic *C. elegans* tissues, 12 of which lack the polyQ motif (Nollen et al., 2004; Fig. 6 C and

Table S4). Among these were two CCT subunits of the TRiC chaperonin, which normally promote assembly or maintenance of both solid granules and semiliquid grPBs (Fig. 6, D and E; and Table S2). In yeast, CCT subunits suppress PB formation and may interact with polyQ aggregates of RNP factors (Nadler-Holly et al., 2012). Furthermore, human CCT proteins cross-link to mRNA in live HeLa cells (Castello et al., 2012). Thus, regulation of polyQ-containing IDR interactions may control normal RNP coassembly dynamics in vivo with divergent outcomes. Q35 regulators were also significantly enriched among P granule modulators (Fig. 6 C), suggesting these may be broadly involved in large-scale coassembly.

RNP granule modulators reveal mRNA repression by multiple regulators

Previous studies suggested that grPB dynamics are tied to translational repression (Noble et al., 2008; Hubstenberger et al., 2013). To further test this connection, all solid granule modulators were depleted in a set of 21 transgenic strains that express *gfp:his-11* reporter mRNAs regulated by different 3' UTRs (Fig. 7; Merritt et al., 2008). The 3' UTR reporters include some known RBP targets and recapitulate various spatiotemporal translation patterns mediated by RBPs (Fig. 7 A; Merritt et al., 2008). RNAi of 22/66 solid modulators strongly increased GFP levels from one or more reporters (17) or weakly increased GFP from at least two reporters (5), revealing genes that repress expression (Figs. 7 B and S2). Depletion of 20 genes decreased GFP from various reporters indicating factors that activate or support expression (Fig. S2). Some repressive genes fell into both classes; RNAi de-repressed some reporters but reduced expression of others (Figs. 7 B and S2). Thus, modifiers of solid granules are enriched for regulators of mRNA activity or levels.

Repressive genes affected subsets of 3' UTR reporters in different stages of oogenesis. In late stages (proximal gonad), two overlapping reporter subsets were de-repressed after loss of PUF-5, PUF-3, or both (Fig. 7 B). This "PUF group" included known mRNA targets specific to PUF-5 (*fog-1* and *glp-1*) or PUF-3 (*nos-3*) or corepressed by both (*pos-1* and *spn-4*; Lublin and Evans, 2007; Stumpf et al., 2008; Hubstenberger et al., 2012). Several potential new PUF-sensitive 3' UTRs were also revealed (Fig. 7 B). A "GLD-1 group" was defined by GLD-1-sensitive 3' UTRs that were de-repressed in early stages (distal gonad) and included previously established or predicted GLD-1 targets (Fig. 7 B; Lee and Schedl, 2001; Jungkamp et al., 2011; Wright et al., 2011; Doh et al., 2013). These results support reporter screen accuracy, with some false negatives based on previous quantifications (Hubstenberger et al., 2012). Loss of multiple granule modulators de-repressed these same 3' UTR reporters in proximal oocytes, distal gonads, or both, indicating they function with PUF-5, PUF-3, and/or GLD-1 directly or indirectly (Fig. 7 B and Table 1). Some repressive genes acted on 3' UTRs insensitive to these known RBPs, suggesting they may also function with as yet unknown RBP repressors (Fig. 7 B). Unexpectedly, reporter screens also revealed a possible new domain of mRNA repression during midmeiosis. RNAi of the RRM protein DAZ-1 and three other genes uniquely de-repressed *fog-1* and *lip-1* reporters within the late-distal to medial gonad, which was spatially distinct from control of these same reporters by GLD-1 in earlier stages and by PUF-5 in later oocytes (Fig. 7, C–F). DAZ-1 loss did not increase *fog-1* reporter mRNA levels consistent with control of translation (Fig. 7 G). These re-

porter activations could be an indirect consequence of meiotic progression defects, a known *daz-1* phenotype (Karashima et al., 2000). However, progression defects were not obvious in our temporally limited RNAi conditions. In addition, this subgroup only repressed a few reporters, indicating mRNA specificity (Fig. 7 B). Therefore, it is possible that a DAZ-1-dependent mRNA control system functions during midmeiosis. Regardless, these data reveal the remarkable intricacies of translation patterning in oogenesis and new genes that participate in this regulation.

Several RNA-associated proteins (RAPs) suggest corepression of mRNA translation by different mechanisms. RNAi of IFET-1 (4E-T homologue), ATX-2 (Ataxin2-related protein), CAR-1 (Lsm14 homologue), and LET-711/Not1 strongly de-repressed several 3' UTR reporters (Fig. 7, B and K). ATX-2 loss did not increase levels of two of three mRNAs tested, whereas IFET-1 loss caused only small mRNA level increases, supporting roles primarily in translational repression (Fig. 7 H). LET-711/Not1 loss reduced *fog-1* mRNA levels and suppressed GFP activity of several reporters, suggesting possible functions in both mRNA maintenance and translational repression (Fig. 7, B and L). These findings are consistent with previous work that also identified mRNAs repressed by these RAPs (Ciosk et al., 2004; Gallo et al., 2008; Noble et al., 2008; Sengupta et al., 2013). However, the broad 3' UTR survey here showed interesting new relationships with RBP repressors. Most 3' UTR reporters (5/6) strongly repressed by PUF-5 and/or PUF-3 in oocytes also required two or more of these RAPs, as did 9/21 reporters overall (Fig. 7 B). Specific 3' UTRs varied in sensitivity to RAP depletion. IFET-1 repressed multiple reporters in the PUF group, GLD-1 group, and others, supporting that IFET-1 is a broad-based corepressor throughout germline development (Li et al., 2009; Guven-Ozkan et al., 2010; Sengupta et al., 2013). ATX-2 strongly repressed reporters controlled by PUF-5 and PUF-3 in late oogenesis stages, revealing a new important function of ATX-2 in PUF-mediated mRNA repression (Fig. 7 B). LET-711/Not1 repressed some of the same mRNAs but also two reporters (*fbf-1* and *fbf-2*) that were insensitive to PUFs and other RAPs. If poly(A) tail removal contributes to LET-711/Not1 repression, then GLD-2 poly(A) polymerase may counter this function. In support of this, both *fog-1* and *glp-1* reporter activities were reduced by *gld-2* RNAi without alteration of mRNA levels under these conditions (Fig. 7, B and I–L). Collectively, therefore, these results suggest that repression of many mRNAs requires three or more repressive factors: an mRNA-specific RBP and at least two RAPs. Because the four RAPs found here likely mediate different molecular activities, multiple mechanisms may combine to repress many mRNAs, either independently or in dependent pathways initiated by mRNA-specific RBPs.

mRNA repression systems control grPBs and solid granules

Comparison of repressive gene effects on reporters, semiliquid grPBs, and solid granules suggests relationships between mRNA regulation and granule dynamics (Table 1). PUF-5, PUF-3, and several RAP corepressors (ATX-2, IFET-1, and CAR-1) repressed overlapping 3' UTR reporters and were all necessary for normal grPB formation in arrested oocytes (Tables 1 and S3). Similarly, GLD-1, DAZ-1, and the same RAPs also promoted grPB formation in the distal to medial germline

Discussion

This study reveals new features of the intricate networks that control RNP dynamics and mRNA repression during *C. elegans* oogenesis. RNA-binding repressors work with multiple corepressor factors to repress translation of mRNAs. These repression systems also induce RNP competence for large-scale condensation into semiliquid or solid states with dynamics that may be modulated by polyQ containing disordered domains in RNPs. Surprisingly, polyadenylation factors contribute to this pathway by stimulating rather than inhibiting condensation of repressed mRNPs. Our study also revealed several unexpected regulatory pathways that influence these mRNP transformation systems, including signaling systems, chaperone activities, membrane trafficking, and nuclear control pathways.

mRNA controls and polyQ factors regulate RNP coassembly dynamics

Both semiliquid grPB coalescence and solid granule formation depend on multiple repression mediators and regulators. This finding suggests RNPs are “licensed” for coassembly by translational repression systems, leading to large-scale condensation or polymerization when induced. In one model, mRNAs bind sequence-specific RBPs, which recruit cofactors with multivalent interaction domains that will drive condensation upon oogenesis arrest or polymerization when CGH-1 helicase is inactivated. Alternatively, RBPs and corepressors might induce repressed mRNP states that permit binding or alteration of condensation factors on mRNAs. PolyQ-containing IDRs could mediate these interactions, modulate fluidity, or specify sorting within grPBs. In support of this idea, IDRs common to RBPs can drive condensation *in vitro*, and polyQ/N motifs prevalent in some fungal and somatic RNP granule proteins influence co-

assembly (Gilks et al., 2004; Decker et al., 2007; Reijns et al., 2008; Kato et al., 2012; Lee et al., 2013; Toretzky and Wright, 2014). Some repressive factors may instead control expression of key condensation regulators, leading to specific dynamics and organization in different RNP bodies.

The functions of poly(A) tail regulators in grPB dynamics are counterintuitive given their expected effects on translation. Poly(A) controls could act indirectly by altering expression of various regulators or by global shifts in mRNA levels or pools of repressed mRNAs. Alternatively, they could play more specific novel roles, an idea consistent with several observations. PAB-1 and CCF-1 are prominent grPB components (Jud et al., 2008; Hubstenberger et al., 2013). In addition, PAB-1 binds ATX-2, which promotes grPB formation and repression (this study; Ciosk et al., 2004; Maine et al., 2004). In other organisms, the Not1 scaffold recruits CCF-1 and CCR-4 to mRNAs, a function likely conserved in *C. elegans* (Nousch et al., 2013; Panepinto et al., 2013; Shirai et al., 2014). Further, mammalian Not1 can bind directly to the CGH-1 ortholog Ddx6 and stimulates ATPase activity (Chen et al., 2014; Mathys et al., 2014; Rouya et al., 2014). Thus, two intriguing possibilities are raised. Repressed mRNPs may need sufficient PAB-1 loaded on poly(A) tails to promote coalescence and/or slow exit from grPBs while preventing PAB-mediated stimulation of translation. Perhaps ATX-2 plays some role in these activities. In addition, LET-711/Not1 may prevent solidification by direct recruitment and activation of the CGH-1 RNA helicase, given their common phenotypes. It could be that Not1 modulation of both polyadenylation and CGH-1 helicase collaborate to tune multivalent interactions among RNPs.

Several genes inhibit square sheet formation, suggesting roles in preventing solidification as shown for LET-711/Not1 and CGH-1. Interestingly, genes that support global mRNA produc-

Table 1. Summary of repressive gene phenotypes

Gene ^a	Sequence	Protein description ^b	Repression group ^c	grPB phenotype ^d	<i>cgh-1</i> solid phenotype ^e	PolyQ motif
<i>puf-5</i>	F54C9.8	RBP, (PUF)	PUF	Disrupt (I)	Suppress	–
<i>puf-3</i>	Y45F10A.2	RBP, (PUF)	PUF	Disrupt (I)	Suppress	–
<i>atx-2</i>	D2045.1	RAP, PAB binding (Lsm, PAM)	PUF, GLD, other	Disrupt (I)	Suppress	+
<i>ifet-1</i>	F56F3.1	RAP, 4E binding (4E-T)	PUF, GLD, other	Disrupt (I)	Suppress	+
<i>car-1</i>	Y18D10A.17	RAP, (Lsm14, FDF)	PUF, GLD, other	Disrupt (I)	Suppress	+
<i>let-711</i>	F57B9.2	RAP, deadenylation scaffold (Not1)	PUF, GLD, other	Squares (II)	Enhance	+
<i>let-60</i>	ZK792.6	Small G protein (Ras)	PUF, other	None	Suppress	–
<i>lin-3</i>	F36H1.4	Ligand, Ras signal ligand (EGF)	PUF	Disrupt (I)	Suppress	–
<i>hda-1</i>	C53A5.3	Histone deacetylase (HDAC)	PUF	None	Suppress	–
<i>vha-10</i>	F46F11.5	Vacuolar ATPase subunit	PUF, other	Large (II)	Enhance	–
<i>pigv-1</i>	T09B4.1	GPI mannosyl transferase	PUF, GLD, other	None	Suppress	–
-	C50E3.12	E3 ubiquitin ligase	PUF	Variable	Suppress	–
<i>gld-1</i>	T23G11.3	RBP (KH)	GLD	Disrupt (I)	Suppress	–
<i>daz-1</i>	F56D1.7	RBP, (RRM)	DAZ	Disrupt (I)	Suppress	–
<i>teg-4</i>	K02F2.3	RAP, snRNP factor (Sf3B3)	DAZ	Squares (III)	High diffuse	–
-	M28.5	RAP, snoRNP factor (Nhp2)	DAZ	Squares (II)	High diffuse	–
<i>eftu-2</i>	ZK328.2	RAP, snRNP factor (SNU114)	DAZ	Squares (II)	High diffuse	–

^aGenes that showed strong de-repression of at least one 3' UTR reporter after RNAi, as in Fig. 7 B.

^bRBP is a sequence-specific RNA-binding protein based on evidence or RNA-binding domain homology; RAP is an RNA-associated protein that associates with RNAs either indirectly or directly based on evidence or homologies. Terms in parentheses indicate predicted domains and homologies.

^cRepression groups as defined in Fig. 7 B and text.

^d"Disrupt" denotes RNAi-induced dissolution and/or reduced grPB sizes, which are class I (I) phenotypes; "squares" denote square granule formation, a class II phenotype (II); "large" denotes enlarged and more grPBs; "variable" refers to different gonads resembling either class I or II; "none", no defect. See Table S3 for additional phenotype descriptions and gonad regions affected.

^e"Suppress" denotes disruption or reduced numbers of square granules; "enhance" denotes increased square granule numbers and/or sizes; "high diffuse" denotes similar numbers of square granules with increased diffuse GFP:CAR-1. See Table S2 for additional phenotype descriptions and gonad regions affected.

tion or export (and broad reporter expression) are enriched in this class (Table S2 and Fig. S2). Further, CGH-1 promotes mRNA stability of regulated germline mRNAs (Boag et al., 2008). Potentially, mRNAs may stimulate liquidity of native RNP bodies. In support of this idea, RNA increases fluidity of liquid RNP droplets in vitro (Elbaum-Garfinkle et al., 2015). LET-711/Not1-activated CGH-1 helicase could specifically act on repressed mRNPs in part to retain mRNAs, preventing solid polymerization of mRNP-bound coassembly proteins like CAR-1. If so, the opposing activity of GLD-2 poly(A) polymerase in supporting condensation is likely independent of its known role in promoting widespread mRNA stability (Nousch et al., 2014).

Translational repression by multiple mechanisms

Predicted and known functions of corepressor RAPs suggest that mRNA-specific RBP repressors may induce or cooperate with several different repression mechanisms. IFET-1 can bind translation initiation factor eIF4E and thus may inhibit initiation at mRNA 5' ends (Li et al., 2009). ATX-2 binds PAB-1, and thus could potentially control PAB at mRNA 3' ends (Ciosk et al., 2004; Maine et al., 2004). In other species, ATX-2 homologues also directly bind mRNAs and control mRNA stability or translation, but on sequences likely distinct from known PUF or GLD-1 sites in *C. elegans* mRNAs (McCann et al., 2011; Zhang et al., 2013; Yokoshi et al., 2014). LET-711/Not1 is a scaffold that recruits deadenylases and CGH-1/Ddx6, in other species and likely *C. elegans* (Nousch et al., 2013; Panepinto et al., 2013; Inada and Makino, 2014; Shirai et al., 2014; Temme et al., 2014). A divergent yeast CAR-1 homologue inhibits eIF4G function (Rajyaguru et al., 2012). Therefore, these RAPs likely inhibit translation by different mechanisms. Given common mRNA targets with PUF-3, PUF-5, and GLD-1, these RAPs work with mRNA-specific RBPs to repress translation. RBPs could recruit multiple RAPs, or some RAPs could act independently on the same mRNAs. Regardless, these findings suggest a flexible “multiple mechanism” scenario: Single RBP complexes or combinations bound at different RNA sites could target several steps of translation. With variations in relative recruitments or activities, different RAP-driven processes may predominate for certain mRNAs or at specific stages. Combined multiple mechanisms could be widespread, which could explain ongoing controversies over RBP and miRNA mechanisms in other systems. Depending on different cell states or time in development, the predominance of a given mechanism could change.

Conserved novel pathways regulate RNP dynamics and pathological states

The more unexpected genes from our screen implicate molecular chaperones, intracellular trafficking, and nuclear RNA pathways in RNP body formation or metabolism. Although these genes could act indirectly, some observations hint at potentially specific roles. First, grPB control by several nuclear transport and membrane trafficking factors could relate to direct physical and functional links found between nuclear pores, membranes, and RNP granules in the germline and embryo (Pitt et al., 2000; Sheth et al., 2010; Voronina and Seydoux, 2010; Patterson et al., 2011). In addition, some of these genes are homologues to human proteins that cross-link to RNAs in vivo, suggesting more direct influences on RNA control (Castello et al., 2012). We also identified mRNA processing factors. Intriguingly, sev-

eral of the same genes influence miRNA and siRNA pathways, and phylogenetic analyses argue these genes may have adapted roles that coevolved with small RNA controls (Tabach et al., 2013). Perhaps, these adapted functions impact other aspects of RNP dynamics. A common feature of RNPs is their capacity for large-scale coassembly, which is tightly regulated in vivo. Thus, these modifiers may contribute to RNP dynamics in other systems. If so, we predict functional variations with different cell and RNP granule types. In support of this, the CCT complex promotes RNP coassembly in oocytes but suppresses Q35 aggregation in somatic cells and PB formation in yeast (Nollen et al., 2004; Nadler-Holly et al., 2012). These contrasting activities could reflect different RNP body properties, different cell and developmental states, or both.

RNP modulators may broadly modulate pathologies tied to inappropriate RNP aggregation, analogous to RNP solids in nematode helicase mutants. Interestingly, two genes found here (ATX-2 and alfa-1) are homologues of human genes (Ataxin-2 and c9orf72) commonly mutated in three human neurodegenerative disorders (frontotemporal dementia, amyotrophic lateral sclerosis, and spinocerebellar ataxia type 2), which exhibit abnormal RNP-rich aggregates (Lastes-Becker et al., 2008; Elden et al., 2010; Heutink et al., 2014; Lattante et al., 2014). ATX-2 and homologues control mRNA translation and stability (this study; Ciosk et al., 2004; McCann et al., 2011; Zhang et al., 2013; Yokoshi et al., 2014). Functions of c9orf72 may include membrane vesicle trafficking (Farg et al., 2014). It is also intriguing that these disorders often result from polyQ expansion mutations, given the prevalence of polyQ motifs among RNP granule proteins. Effects of polyQ expansion are controversial and include the possibility of repeat-derived toxic peptides or RNA independent of gene function (Heutink et al., 2014; Mizielinska and Isaacs, 2014). However, our studies support roles for these seemingly unrelated proteins and numerous other polyQ factors in regulation of physiological RNP dynamics. Therefore, future studies could reveal new insights into how larger-scale RNP organization is controlled in normal and pathological states and their connections to RNP function.

Materials and methods

Strains and RNAi vectors

Strains were maintained by standard methods (Brenner, 1974). The following strains and alleles were used (for transgenes, p_{gene} = promoter and UTR^{gene} = 3' UTR from specified genes): N2 (Bristol wild-type strain); CB4108 (*fog-2(q71)*); TE71 (*fog-2(q71)*); $p_{pie-1}::car-1::gfp::UTR^{pie-1}$; $p_{nmy-2}::pgl-1::mrfp$; TE81 (*cgh-1(tm691ts)*); $p_{pie-1}::car-1::gfp::UTR^{pie-1}$; Hubstenberger et al., 2013). Strains expressing *gfp::h2b* 3' UTR reporter mRNAs were generated by Merritt et al. (2008) and included: JH2270, $p_{pie-1}::gfp::h2b::UTR^{h2b-1}$; JH2296, $p_{pie-1}::gfp::h2b::UTR^{h2b-2}$; JH2207, $p_{pie-1}::gfp::h2b::UTR^{fog-2}$; JH2423, $p_{pie-1}::gfp::h2b::UTR^{fog-1}$; JH2436, $p_{pie-1}::gfp::h2b::UTR^{gld-1}$; JH2252, $p_{pie-1}::gfp::h2b::UTR^{gfp-1}$; JH2377, $p_{pie-1}::gfp::h2b::UTR^{mes-3}$; JH2221, $p_{pie-1}::gfp::h2b::UTR^{mes-5}$; JH2200, $p_{pie-1}::gfp::h2b::UTR^{nos-3}$; JH2320, $p_{pie-1}::gfp::h2b::UTR^{pgl-1}$; JH2349, $p_{pie-1}::gfp::h2b::UTR^{pgl-3}$; JH2427, $p_{pie-1}::gfp::h2b::UTR^{pos-1}$; JH2311, $p_{pie-1}::gfp::h2b::UTR^{spm-4}$; JH2297, $p_{pie-1}::gfp::h2b::UTR^{tbb-2}$; JH2236, $p_{pie-1}::gfp::h2b::UTR^{pal-1}$; JH2379, $p_{pie-1}::gfp::h2b::UTR^{rme-1}$; JH2333, $p_{pie-1}::gfp::h2b::UTR^{mes-3}$; JH2313, $p_{pie-1}::gfp::h2b::UTR^{rme-2}$; JH2267, $p_{pie-1}::gfp::h2b::UTR^{lip-1}$; JH2220, $p_{pie-1}::gfp::h2b::UTR^{par-5}$; JH2223, $p_{pie-1}::gfp::h2b::UTR^{daz-1}$. Strains were provided by the *Caenorhabditis* Genetics Center (Minneapolis, MN), except for *cgh-1(tm691)*

strains generously provided by D. Greenstein (University of Minnesota, Minneapolis, MN). For the primary RNAi screen and most secondary assays, RNAi feeding vectors in L4440 backbones were derived from the *C. elegans* RNAi genome library (Kamath and Ahringer, 2003; Source Bioscience). An *ifet-1(RNAi)* feeding vector (pTE7.70) was made carrying full-length open reading frame of *ifet-1* cDNA in L4440. For some experiments, *puf-5* RNAi vector pTE7.30 (full-length *puf-5* cDNA in L4440) and *puf-3* RNAi vector pTE7.60 (15–610 of *puf-3* cDNA in L4440) were used, as described previously (Hubstenberger et al., 2012). For all RNAi vectors that gave positive phenotypes, inserts were sequenced by the University of Colorado Cancer Center DNA Sequencing and Analysis Center. Only RNAi vectors that gave clean single sequences were included in analyses; RNAi bacteria that gave mixed sequences were either not included or vectors were recloned, sequenced, and retested. A nonspecific empty L4440 vector was used as a negative control in all RNAi experiments (control or *mock(RNAi)*), as described previously (Timmons et al., 2001; Hubstenberger et al., 2012).

RNAi screens

RNAi was done by feeding (Kamath and Ahringer, 2003), with the following modifications. Hermaphrodites were bleach treated, and embryos were allowed to hatch on unseeded plates for 20–40 h to synchronize as L1 larvae. L1 larvae were transferred to standard bacteria (OP-50) plates and grown at 15°C for 20–24 h and then shifted to 20°C for 20–24 h until late L3 to early L4 stages. L3/L4 larvae were washed three times in M9 with 50 µg/ml carbenicillin and were then transferred onto RNAi plates at 20°C. RNAi plates were freshly prepared by growing HT115 RNAi clones in Luria broth (LB) + 25 µg/ml carbenicillin at 37°C for 16 h, placing clones on ice for 6–7 h, adding IPTG to 1 mM, and then seeding and growing RNAi plates at 20–23°C (RT) for 16–20 h (Noble et al., 2008; Hubstenberger et al., 2013). RNAi plates were grown to young adults at 20°C (20–24 h) and then transferred to 25°C for 16–20 h. Adults were transferred to microscope slides and assayed by epifluorescence or confocal microscopy (see following section). For each screen and experiment, phenotypes were analyzed in ≥40 worms for each RNAi. This temporally restricted protocol induces strong loss of at least some proteins (CAR-1 and PUF-5) in adult germlines that make oocytes but in general bypasses known gene functions in germ cell proliferation and sex determination (data not shown).

A sublibrary was screened for modifiers of square sheet granules marked with GFP:CAR-1 in *cgh-1(tm691ts)* animals by fluorescence microscopy (described below). This sublibrary combined two sets of genes: (a) genes controlling embryo sensitivity to osmotic stress (embryo osmotic integrity phenotype; Sönnichsen et al., 2005; WormBase, WBPhenotype:0000365) and (b) genes with oogenesis-enriched expression, as described previously (Reinke et al., 2004). After removing inviable or contaminated clones, a total of 999 nonoverlapping genes were tested (Table S1). For the primary screen in *cgh-1(tm691)*, RNAi clones were scored as solid modulators if ≥20% of worms ($n \geq 40$) showed obvious alterations in square sheet granules (Table S2). All positive RNAi phenotypes were confirmed in at least two independent experiments, and RNAi clone sequences confirmed as described above. Negative clones were only tested once, with exception of *dcap-2*, which was tested twice.

Two secondary RNAi screens were done on 66 primary screen positives. To test impacts on normal germline RNP bodies, RNAi depletions were done in arrested *fog-2(q71);gfp:car-1;pgl-1::rfp* females; unmated female L4 larvae were directly transferred to RNAi plates and grown to produce adult females that lack sperm but are otherwise wild type in control RNAi, as described (Noble et al., 2008; Hubstenberger et al., 2013). To test control through mRNA 3' UTRs, positives were RNAi depleted in transgenic hermaphrodites

carrying *gfp:H2B* 3' UTR reporters and screened by fluorescence microscopy. For 3' UTR reporter assays, increases in GFP:H2B expression were defined as weak (light red in heatmaps) if 10–30% animals had fluorescence above control, medium (mild red) if >30% have a fluorescence higher than control, and strong (hot red) if >60% of analyzed worms had higher levels than mock and at least 30% had fluorescence five times higher than mock. Decreases in GFP:H2B (blue in heatmaps) were defined similarly. Quantification of GFP:H2B was done as described previously (Hubstenberger et al., 2012); maximum intensity was determined in lines drawn across nuclei minus cytoplasmic background from epifluorescence images using Axiovision 4.6.3 (Carl Zeiss) and ImageJ (described below). For each experiment, animals from different RNAi treatments were processed in parallel, with identical UV intensities, exposure times, and adjustments.

Immunofluorescence and in situ hybridization

For immunofluorescence (IF), adult animals were dissected and frozen on slides under coverslips on dry ice, coverslips removed, fixed in cold methanol, and blocked in PBS with 0.5% BSA as described previously (Noble et al., 2008). Primary antibodies used were rabbit anti-CGH-1 (CB3770 5.6S; gift of D. Greenstein) and rabbit anti-GFP (Life Tech, A-6455). Simultaneous fluorescence in situ hybridization and IF (FISH-IF) was done as described previously (Noble et al., 2008). Worms were dissected on slides and frozen (as above) and fixed in serial methanol dilutions (100%, 90%, 70%, and 50%). After air drying, slides were incubated in PBS with 0.5% BSA, refixed in fresh 4% formaldehyde in PBS, washed in PBS with 2 mg/ml glycine, and preincubated in hybridization buffer (50% formamide, 5XSSC, 100 µg/ml salmon sperm DNA, and 0.01% Tween 20) at 50°C for 1 h. Digoxigenin-labeled RNA probes to *pos-1* mRNA in hybridization buffer were hybridized at 50°C overnight. Slides were then washed at 50°C over 5 h in wash buffer (50% formamide, 5XSSC, and 0.01% Tween 20), 2XSSC at RT and finally in PBS with 0.5% BSA. Probes were detected with Fluorescent Antibody Enhancer Set for DIG Detection (Roche) using Cy3-labeled mouse antidigoxigenin antibody (Jackson ImmunoResearch Laboratories), and proteins were detected with primary antibodies described above and goat anti-rabbit Alexa Fluor 488 secondary antibodies (Life Technologies).

Imaging

Epifluorescence images were acquired at room temperature with a Zeiss Axioskop microscope using a 40x, 1.4 NA plan apochromat oil objective, imaged with AxioCam MRm (Carl Zeiss), and quantified with Axiovision 4.6.3 software (Carl Zeiss). For live epifluorescence imaging, worms were transferred to 2% agarose pads in M9 buffer with 30 mM NaN₃. For IF and FISH-IF of fixed gonads (described below), slides were mounted in Prolong Gold mounting medium (Life Technologies). For confocal microscopy, a Leica TCS SP5 II confocal microscope fluorescence was used at 20–22°C with HCX plan apochromat CS 40x oil objective, 1.25 aperture, using Leica image acquisition software. For single confocal sections of FISH-IF slides, 1 Airy unit pinhole was used. For FRAP on Leica TCS SP5 II confocal microscope, animals were mounted on 2% agarose pads in M9 buffer with 2% Tricaine methanesulfonate and 0.2% tetramisole hydrochloride (Sigma-Aldrich), 2-µm circular zones were photobleached, and confocal time series were recorded at minimal laser intensities, using 2 Airy unit pinhole size (Hubstenberger et al., 2013). For image analyses, ImageJ and the plugin collection MBF "ImageJ for Microscopy" by Tony Collins were used. Fluorochromes were EGFP and mRFP (for live imaging), Alexa Fluor 488, Alexa Fluor 594 (for IF), and Cy3 (for FISH).

RNA quantification

100 worms were washed twice with M9 and once with cold ddH₂O. RNA was extracted using Trizol LS (Invitrogen). cDNAs were generated using random hexamers with the Superscript III First-Strand Synthesis System (Invitrogen). Real-Time PCR was performed in triplicate using SYBR Green Reagent on a StepOnePlus Real-Time PCR System (Applied Biosystems). Primers were designed around exon–exon junctions to avoid amplification of contaminant genomic DNA using the Primer Express 3.0 software. For *gfp*, we used primers 5′-AGGTGATG CAACATACGGAAA-3′ and 5′-AAGCATTGAACACCATAACAG-3′. For *act-1*, we used primers 5′-TTGCCCATCAACCATGAA-3′ and 5′-CCGATCCAGACGGAGTACTTG-3′. Results were analyzed using the StepOne Software v2.1 (Applied Biosystems). Relative mRNA levels were calculated using the Quantitation Comparative CT ($\Delta\Delta CT$) method and normalized to actin mRNA levels. Results were confirmed for at least two independent RNAi experiments.

Bioinformatics

Screen positives were linked to possible functions initially using NCBI COG annotations, and second by direct domain inspection. To test enrichment specificity of NCBI COG gene functions, two functional categories were generated and compared by (1) DNA control genes, by pooling together codes B, L, K, and Y (Chromatin Structure and dynamics, Replication and repair, Transcription, and Nuclear structure); and (2) RNA control genes, by pooling codes A and J (RNA processing and modification and Translation, ribosomal structure, and biogenesis; Tatusov et al., 2003). To search for common motifs, MEME was used (Bailey and Elkan, 1994). Motif frequency statistics were further analyzed both in the tested library and screen positives using FIMO (Grant et al., 2011). Gene clustering on heatmaps was generated using the one minus Pearson correlation (GENE-E). IDRs were predicted using PON DR-FIT (Xue et al., 2010).

Online supplemental material

Fig. S1 shows that ATX-2 and GLD-2 depletion disrupts coassembly of grPB components CGH-1 and *pos-1* mRNA, in addition to CAR-1. Fig. S2 shows 3′ UTR reporter expression changes for all genes that increase or decrease expression after RNAi. Tables S1–S4 are Excel spreadsheets. Table S1 lists all 999 genes in the total RNAi sublibrary that was screened for modulation of solid granules in *cgh-1(tm691)*. Table S2 lists all genes that altered solid granules in *cgh-1(tm691)*, and genes from prior P granule modifier screen (Updike and Strome, 2009) that were present in the starting library, including those not found in the solid granule screen. Table S3 lists effects of all solid modifiers on grPBs, P granules, and oocytes in normal arrested gonads. Table S4 lists solid granule modifiers that were also found as Q35 aggregation suppressors by Nollen et al. (2004). Online supplemental material is available at <http://www.jcb.org/cgi/content/full/jcb.201504044/DC1>.

Acknowledgments

We thank David Greenstein for providing antibodies, *cgh-1(tm691)* strains, and detailed information. We also thank Rytis Prekeris, Chad Pearson, Natalia Toledo, and Richard Davis for discussions. Most strains were provided by the *Caenorhabditis* Genetics Center (Minneapolis, MN), which is funded by National Institutes of Health Office of Research Infrastructure Programs (P40 OD010440).

This work was supported by grants from the National Institutes of Health (GM79682 to T.C. Evans), the National Science Foundation (IOS-0725416 to T.C. Evans), and the Fondation pour la Recherche Médicale (Code FRM: SPF20130526681 to A. Hubstenberger).

The authors declare no competing financial interests.

Submitted: 10 April 2015

Accepted: 25 September 2015

References

- Arur, S., M. Ohmachi, M. Berkseth, S. Nayak, D. Hansen, D. Zarkower, and T. Schedl. 2011. MPK-1 ERK controls membrane organization in *C. elegans* oogenesis via a sex-determination module. *Dev. Cell.* 20:677–688. <http://dx.doi.org/10.1016/j.devcel.2011.04.009>
- Audhya, A., F. Hyndman, I.X. McLeod, A.S. Maddox, J.R. Yates III, A. Desai, and K. Oegema. 2005. A complex containing the Sm protein CAR-1 and the RNA helicase CGH-1 is required for embryonic cytokinesis in *Caenorhabditis elegans*. *J. Cell Biol.* 171:267–279. <http://dx.doi.org/10.1083/jcb.200506124>
- Bailey, T.L., and C. Elkan. 1994. Fitting a mixture model by expectation maximization to discover motifs in biopolymers. *Proc. Int. Conf. Intell. Syst. Mol. Biol.* 2:28–36.
- Boag, P.R., A. Nakamura, and T.K. Blackwell. 2005. A conserved RNA-protein complex component involved in physiological germline apoptosis regulation in *C. elegans*. *Development.* 132:4975–4986. <http://dx.doi.org/10.1242/dev.02060>
- Boag, P.R., A. Atalay, S. Robida, V. Reinke, and T.K. Blackwell. 2008. Protection of specific maternal messenger RNAs by the P body protein CGH-1 (Dhh1/RCK) during *Caenorhabditis elegans* oogenesis. *J. Cell Biol.* 182:543–557. <http://dx.doi.org/10.1083/jcb.200801183>
- Brangwynne, C.P., C.R. Eckmann, D.S. Courson, A. Rybarska, C. Hoegge, J. Gharakhani, F. Jülicher, and A.A. Hyman. 2009. Germline P granules are liquid droplets that localize by controlled dissolution/condensation. *Science.* 324:1729–1732. <http://dx.doi.org/10.1126/science.1172046>
- Brangwynne, C.P., T.J. Mitchison, and A.A. Hyman. 2011. Active liquid-like behavior of nucleoli determines their size and shape in *Xenopus laevis* oocytes. *Proc. Natl. Acad. Sci. USA.* 108:4334–4339. <http://dx.doi.org/10.1073/pnas.1017150108>
- Brenner, S. 1974. The genetics of *Caenorhabditis elegans*. *Genetics.* 77:71–94.
- Buchan, J.R. 2014. mRNP granules. Assembly, function, and connections with disease. *RNA Biol.* 11:1019–1030. <http://dx.doi.org/10.4161/15476286.2014.972208>
- Budirahardja, Y., T.D. Doan, and R. Zaidel-Bar. 2015. Glycosyl phosphatidylinositol anchor biosynthesis is essential for maintaining epithelial integrity during *Caenorhabditis elegans* embryogenesis. *PLoS Genet.* 11:e1005082. <http://dx.doi.org/10.1371/journal.pgen.1005082>
- Castello, A., B. Fischer, K. Eichelbaum, R. Horos, B.M. Beckmann, C. Strein, N.E. Davey, D.T. Humphreys, T. Preiss, L.M. Steinmetz, et al. 2012. Insights into RNA biology from an atlas of mammalian mRNA-binding proteins. *Cell.* 149:1393–1406. <http://dx.doi.org/10.1016/j.cell.2012.04.031>
- Chen, Y., A. Boland, D. Kuzuoğlu-Öztürk, P. Bawankar, B. Loh, C.T. Chang, O. Weichenrieder, and E. Izaurralde. 2014. A DDX6-CNOT1 complex and W-binding pockets in CNOT9 reveal direct links between miRNA target recognition and silencing. *Mol. Cell.* 54:737–750. <http://dx.doi.org/10.1016/j.molcel.2014.03.034>
- Ciosk, R., M. DePalma, and J.R. Priess. 2004. ATX-2, the *C. elegans* ortholog of ataxin 2, functions in translational regulation in the germline. *Development.* 131:4831–4841. <http://dx.doi.org/10.1242/dev.01352>
- Decker, C.J., and R. Parker. 2012. P-bodies and stress granules: possible roles in the control of translation and mRNA degradation. *Cold Spring Harb. Perspect. Biol.* 4:a012286. <http://dx.doi.org/10.1101/cshperspect.a012286>
- Decker, C.J., D. Teixeira, and R. Parker. 2007. Edc3p and a glutamine/asparagine-rich domain of Lsm4p function in processing body assembly in *Saccharomyces cerevisiae*. *J. Cell Biol.* 179:437–449. <http://dx.doi.org/10.1083/jcb.200704147>
- Doh, J.H., Y. Jung, V. Reinke, and M.H. Lee. 2013. *C. elegans* RNA-binding protein GLD-1 recognizes its multiple targets using sequence, context, and structural information to repress translation. *Worm.* 2:e26548. <http://dx.doi.org/10.4161/worm.26548>
- Elbaum-Garfinkle, S., Y. Kim, K. Szczepaniak, C.C. Chen, C.R. Eckmann, S. Myong, and C.P. Brangwynne. 2015. The disordered P granule protein LAF-1 drives phase separation into droplets with tunable viscosity and dynamics. *Proc. Natl. Acad. Sci. USA.* 112:7189–7194. <http://dx.doi.org/10.1073/pnas.1504822112>
- Elden, A.C., H.J. Kim, M.P. Hart, A.S. Chen-Plotkin, B.S. Johnson, X. Fang, M. Armakola, F. Geser, R. Greene, M.M. Lu, et al. 2010. Ataxin-2 intermediate-length polyglutamine expansions are associated with

- increased risk for ALS. *Nature*. 466:1069–1075. <http://dx.doi.org/10.1038/nature09320>
- Farg, M.A., V. Sundaramoorthy, J.M. Sultana, S. Yang, R.A. Atkinson, V. Levina, M.A. Halloran, P.A. Gleeson, I.P. Blair, K.Y. Soo, et al. 2014. C9ORF72, implicated in amyotrophic lateral sclerosis and frontotemporal dementia, regulates endosomal trafficking. *Hum. Mol. Genet.* 23:3579–3595. <http://dx.doi.org/10.1093/hmg/ddu068>
- Gallo, C.M., E. Munro, D. Rasoloson, C. Merritt, and G. Seydoux. 2008. Processing bodies and germ granules are distinct RNA granules that interact in *C. elegans* embryos. *Dev. Biol.* 323:76–87. <http://dx.doi.org/10.1016/j.ydbio.2008.07.008>
- Gilks, N., N. Kedersha, M. Ayodele, L. Shen, G. Stoecklin, L.M. Dember, and P. Anderson. 2004. Stress granule assembly is mediated by prion-like aggregation of TIA-1. *Mol. Biol. Cell.* 15:5383–5398. <http://dx.doi.org/10.1091/mbc.E04-08-0715>
- Grant, C.E., T.L. Bailey, and W.S. Noble. 2011. FIMO: scanning for occurrences of a given motif. *Bioinformatics*. 27:1017–1018. <http://dx.doi.org/10.1093/bioinformatics/btr064>
- Güven-Ozkan, T., S.M. Robertson, Y. Nishi, and R. Lin. 2010. zif-1 translational repression defines a second, mutually exclusive OMA function in germline transcriptional repression. *Development*. 137:3373–3382. <http://dx.doi.org/10.1242/dev.055327>
- Han, T.W., M. Kato, S. Xie, L.C. Wu, H. Mirzaei, J. Pei, M. Chen, Y. Xie, J. Allen, G. Xiao, and S.L. McKnight. 2012. Cell-free formation of RNA granules: bound RNAs identify features and components of cellular assemblies. *Cell*. 149:768–779. <http://dx.doi.org/10.1016/j.cell.2012.04.016>
- Heinrich, S.U., and S. Lindquist. 2011. Protein-only mechanism induces self-perpetuating changes in the activity of neuronal Aplysia cytoplasmic polyadenylation element binding protein (CPEB). *Proc. Natl. Acad. Sci. USA*. 108:2999–3004. <http://dx.doi.org/10.1073/pnas.1019368108>
- Heutink, P., I.E. Jansen, and E.M. Lynes. 2014. C9orf72; abnormal RNA expression is the key. *Exp. Neurol.* 262(Pt B):102–110. <http://dx.doi.org/10.1016/j.expneurol.2014.05.020>
- Hubstenberger, A., C. Cameron, R. Shtofman, S. Gutman, and T.C. Evans. 2012. A network of PUF proteins and Ras signaling promote mRNA repression and oogenesis in *C. elegans*. *Dev. Biol.* 366:218–231. <http://dx.doi.org/10.1016/j.ydbio.2012.03.019>
- Hubstenberger, A., S.L. Noble, C. Cameron, and T.C. Evans. 2013. Translation repressors, an RNA helicase, and developmental cues control RNP phase transitions during early development. *Dev. Cell*. 27:161–173. <http://dx.doi.org/10.1016/j.devcel.2013.09.024>
- Hyman, A.A., C.A. Weber, and F. Jülicher. 2014. Liquid-liquid phase separation in biology. *Annu. Rev. Cell Dev. Biol.* 30:39–58. <http://dx.doi.org/10.1146/annurev-cellbio-100913-013325>
- Inada, T., and S. Makino. 2014. Novel roles of the multi-functional CCR4-NOT complex in post-transcriptional regulation. *Front. Genet.* 5:135. <http://dx.doi.org/10.3389/fgene.2014.00135>
- Jalkanen, A.L., S.J. Coleman, and J. Wilusz. 2014. Determinants and implications of mRNA poly(A) tail size—does this protein make my tail look big? *Semin. Cell Dev. Biol.* 34:24–32. <http://dx.doi.org/10.1016/j.semcdb.2014.05.018>
- Jud, M.C., M.J. Czerwinski, M.P. Wood, R.A. Young, C.M. Gallo, J.S. Bickel, E.L. Petty, J.M. Mason, B.A. Little, P.A. Padilla, and J.A. Schisa. 2008. Large P body-like RNPs form in *C. elegans* oocytes in response to arrested ovulation, heat shock, osmotic stress, and anoxia and are regulated by the major sperm protein pathway. *Dev. Biol.* 318:38–51. <http://dx.doi.org/10.1016/j.ydbio.2008.02.059>
- Jungkamp, A.C., M. Stoeckius, D. Mecnas, D. Grün, G. Mastrobuoni, S. Kempa, and N. Rajewsky. 2011. In vivo and transcriptome-wide identification of RNA binding protein target sites. *Mol. Cell.* 44:828–840. <http://dx.doi.org/10.1016/j.molcel.2011.11.009>
- Kamath, R.S., and J. Ahringer. 2003. Genome-wide RNAi screening in *Caenorhabditis elegans*. *Methods*. 30:313–321. [http://dx.doi.org/10.1016/S1046-2023\(03\)00050-1](http://dx.doi.org/10.1016/S1046-2023(03)00050-1)
- Karashima, T., A. Sugimoto, and M. Yamamoto. 2000. *Caenorhabditis elegans* homologue of the human azoospermia factor DAZ is required for oogenesis but not for spermatogenesis. *Development*. 127:1069–1079.
- Kato, M., T.W. Han, S. Xie, K. Shi, X. Du, L.C. Wu, H. Mirzaei, E.J. Goldsmith, J. Longgood, J. Pei, et al. 2012. Cell-free formation of RNA granules: low complexity sequence domains form dynamic fibers within hydrogels. *Cell*. 149:753–767. <http://dx.doi.org/10.1016/j.cell.2012.04.017>
- King, O.D., A.D. Gitler, and J. Shorter. 2012. The tip of the iceberg: RNA-binding proteins with prion-like domains in neurodegenerative disease. *Brain Res.* 1462:61–80. <http://dx.doi.org/10.1016/j.brainres.2012.01.016>
- Lastres-Becker, I., U. Rüb, and G. Auburger. 2008. Spinocerebellar ataxia 2 (SCA2). *Cerebellum*. 7:115–124. <http://dx.doi.org/10.1007/s12311-008-0019-y>
- Lattante, S., S. Millicamps, G. Stevanin, S. Rivaud-Péchéux, C. Moigneu, A. Camuzat, S. Da Barroca, E. Mundwiller, P. Couarch, F. Salachas, et al. French Research Network on FTD and FTD-ALS. 2014. Contribution of ATXN2 intermediary polyQ expansions in a spectrum of neurodegenerative disorders. *Neurology*. 83:990–995. <http://dx.doi.org/10.1212/WNL.0000000000000778>
- Lee, M.H., and T. Schedl. 2001. Identification of in vivo mRNA targets of GLD-1, a maxi-KH motif containing protein required for *C. elegans* germ cell development. *Genes Dev.* 15:2408–2420. <http://dx.doi.org/10.1101/gad.915901>
- Lee, C., H. Zhang, A.E. Baker, P. Occhipinti, M.E. Borsuk, and A.S. Gladfelter. 2013. Protein aggregation behavior regulates cyclin transcript localization and cell-cycle control. *Dev. Cell*. 25:572–584. <http://dx.doi.org/10.1016/j.devcel.2013.05.007>
- Li, P., S. Banjade, H.C. Cheng, S. Kim, B. Chen, L. Guo, M. Llaguno, J.V. Hollingsworth, D.S. King, S.F. Banani, et al. 2012. Phase transitions in the assembly of multivalent signalling proteins. *Nature*. 483:336–340. <http://dx.doi.org/10.1038/nature10879>
- Li, W., L.R. DeBella, T. Guven-Ozkan, R. Lin, and L.S. Rose. 2009. An eIF4E-binding protein regulates katanin protein levels in *C. elegans* embryos. *J. Cell Biol.* 187:33–42. <http://dx.doi.org/10.1083/jcb.200903003>
- Lublin, A.L., and T.C. Evans. 2007. The RNA-binding proteins PUF-5, PUF-6, and PUF-7 reveal multiple systems for maternal mRNA regulation during *C. elegans* oogenesis. *Dev. Biol.* 303:635–649. <http://dx.doi.org/10.1016/j.ydbio.2006.12.004>
- Maine, E.M., D. Hansen, D. Springer, and V.E. Vought. 2004. *Caenorhabditis elegans* atx-2 promotes germline proliferation and the oocyte fate. *Genetics*. 168:817–830. <http://dx.doi.org/10.1534/genetics.104.029355>
- Malinowska, L., S. Kroschwald, and S. Alberti. 2013. Protein disorder, prion propensities, and self-organizing macromolecular collectives. *Biochim. Biophys. Acta*. 1834:918–931. <http://dx.doi.org/10.1016/j.bbapap.2013.01.003>
- Mao, Y.S., B. Zhang, and D.L. Spector. 2011. Biogenesis and function of nuclear bodies. *Trends Genet.* 27:295–306. <http://dx.doi.org/10.1016/j.tig.2011.05.006>
- Mathys, H., J. Basquin, S. Ozgur, M. Czarnocki-Cieciura, F. Bonneau, A. Aartse, A. Dziembowski, M. Nowotny, E. Conti, and W. Filipowicz. 2014. Structural and biochemical insights to the role of the CCR4-NOT complex and DDX6 ATPase in microRNA repression. *Mol. Cell*. 54:751–765. <http://dx.doi.org/10.1016/j.molcel.2014.03.036>
- McCann, C., E.E. Holohan, S. Das, A. Dervan, A. Larkin, J.A. Lee, V. Rodrigues, R. Parker, and M. Ramaswami. 2011. The Ataxin-2 protein is required for microRNA function and synapse-specific long-term olfactory habituation. *Proc. Natl. Acad. Sci. USA*. 108:E655–E662. <http://dx.doi.org/10.1073/pnas.1107198108>
- Merritt, C., D. Rasoloson, D. Ko, and G. Seydoux. 2008. 3' UTRs are the primary regulators of gene expression in the *C. elegans* germline. *Curr. Biol.* 18:1476–1482. <http://dx.doi.org/10.1016/j.cub.2008.08.013>
- Mizielinska, S., and A.M. Isaacs. 2014. C9orf72 amyotrophic lateral sclerosis and frontotemporal dementia: gain or loss of function? *Curr. Opin. Neurol.* 27:515–523. <http://dx.doi.org/10.1097/WCO.0000000000000130>
- Nadler-Holly, M., M. Breker, R. Gruber, A. Azia, M. Gymrek, M. Eisenstein, K.R. Willison, M. Schuldiner, and A. Horowitz. 2012. Interactions of subunit CCT3 in the yeast chaperonin CCT/TRiC with Q/N-rich proteins revealed by high-throughput microscopy analysis. *Proc. Natl. Acad. Sci. USA*. 109:18833–18838. <http://dx.doi.org/10.1073/pnas.1209277109>
- Noble, S.L., B.L. Allen, L.K. Goh, K. Nordick, and T.C. Evans. 2008. Maternal mRNAs are regulated by diverse P body-related mRNA granules during early *Caenorhabditis elegans* development. *J. Cell Biol.* 182:559–572. <http://dx.doi.org/10.1083/jcb.200802128>
- Nollen, E.A., S.M. Garcia, G. van Haften, S. Kim, A. Chavez, R.I. Morimoto, and R.H. Plasterk. 2004. Genome-wide RNA interference screen identifies previously undescribed regulators of polyglutamine aggregation. *Proc. Natl. Acad. Sci. USA*. 101:6403–6408. <http://dx.doi.org/10.1073/pnas.0307697101>
- Nousch, M., and C.R. Eckmann. 2013. Translational control in the *Caenorhabditis elegans* germ line. *Adv. Exp. Med. Biol.* 757:205–247. http://dx.doi.org/10.1007/978-1-4614-4015-4_8
- Nousch, M., N. Techritz, D. Hampel, S. Millionigg, and C.R. Eckmann. 2013. The Cer-4-Not deadenylase complex constitutes the main poly(A) removal activity in *C. elegans*. *J. Cell Sci.* 126:4274–4285. <http://dx.doi.org/10.1242/jcs.132936>
- Nousch, M., A. Yeroslaviz, B. Habermann, and C.R. Eckmann. 2014. The cytoplasmic poly(A) polymerases GLD-2 and GLD-4 promote general gene expression via distinct mechanisms. *Nucleic Acids Res.* 42:11622–11633. <http://dx.doi.org/10.1093/nar/gku838>

- Panepinto, J.C., E. Heinz, and A. Traven. 2013. The cellular roles of Ccr4-NOT in model and pathogenic fungi—implications for fungal virulence. *Front. Genet.* 4:302. <http://dx.doi.org/10.3389/fgene.2013.00302>
- Patterson, J.R., M.P. Wood, and J.A. Schisa. 2011. Assembly of RNP granules in stressed and aging oocytes requires nucleoporins and is coordinated with nuclear membrane blebbing. *Dev. Biol.* 353:173–185. <http://dx.doi.org/10.1016/j.ydbio.2011.02.028>
- Pitt, J.N., J.A. Schisa, and J.R. Priess. 2000. P granules in the germ cells of *Caenorhabditis elegans* adults are associated with clusters of nuclear pores and contain RNA. *Dev. Biol.* 219:315–333. <http://dx.doi.org/10.1006/dbio.2000.9607>
- Rajyaguru, P., M. She, and R. Parker. 2012. Scd6 targets eIF4G to repress translation: RGG motif proteins as a class of eIF4G-binding proteins. *Mol. Cell.* 45:244–254. <http://dx.doi.org/10.1016/j.molcel.2011.11.026>
- Ramaswami, M., J.P. Taylor, and R. Parker. 2013. Altered ribostasis: RNA-protein granules in degenerative disorders. *Cell.* 154:727–736. <http://dx.doi.org/10.1016/j.cell.2013.07.038>
- Reijns, M.A., R.D. Alexander, M.P. Spiller, and J.D. Beggs. 2008. A role for Q/N-rich aggregation-prone regions in P-body localization. *J. Cell Sci.* 121:2463–2472. <http://dx.doi.org/10.1242/jcs.024976>
- Reinke, V., I.S. Gil, S. Ward, and K. Kazmer. 2004. Genome-wide germline-enriched and sex-biased expression profiles in *Caenorhabditis elegans*. *Development.* 131:311–323. <http://dx.doi.org/10.1242/dev.00914>
- Rinn, J., and M. Guttman. 2014. RNA Function. RNA and dynamic nuclear organization. *Science.* 345:1240–1241. <http://dx.doi.org/10.1126/science.1252966>
- Rouya, C., N. Siddiqui, M. Morita, T.F. Duchaine, M.R. Fabian, and N. Sonenberg. 2014. Human DDX6 effects miRNA-mediated gene silencing via direct binding to CNOT1. *RNA.* 20:1398–1409. <http://dx.doi.org/10.1261/rna.045302.114>
- Schisa, J.A. 2014. Effects of stress and aging on ribonucleoprotein assembly and function in the germ line. *Wiley Interdiscip. Rev. RNA.* 5:231–246. <http://dx.doi.org/10.1002/wrna.1204>
- Schisa, J.A., J.N. Pitt, and J.R. Priess. 2001. Analysis of RNA associated with P granules in germ cells of *C. elegans* adults. *Development.* 128:1287–1298.
- Sengupta, M.S., W.Y. Low, J.R. Patterson, H.M. Kim, A. Traven, T.H. Beilharz, M.P. Colaiácovo, J.A. Schisa, and P.R. Boag. 2013. ifet-1 is a broad-scale translational repressor required for normal P granule formation in *C. elegans*. *J. Cell Sci.* 126:850–859. <http://dx.doi.org/10.1242/jcs.119834>
- Sheth, U., J. Pitt, S. Dennis, and J.R. Priess. 2010. Perinuclear P granules are the principal sites of mRNA export in adult *C. elegans* germ cells. *Development.* 137:1305–1314. <http://dx.doi.org/10.1242/dev.044255>
- Shirai, Y.T., T. Suzuki, M. Morita, A. Takahashi, and T. Yamamoto. 2014. Multifunctional roles of the mammalian CCR4-NOT complex in physiological phenomena. *Front. Genet.* 5:286. <http://dx.doi.org/10.3389/fgene.2014.00286>
- Si, K., Y.B. Choi, E. White-Grindley, A. Majumdar, and E.R. Kandel. 2010. Aplysia CPEB can form prion-like multimers in sensory neurons that contribute to long-term facilitation. *Cell.* 140:421–435. <http://dx.doi.org/10.1016/j.cell.2010.01.008>
- Sönnichsen, B., L.B. Koski, A. Walsh, P. Marschall, B. Neumann, M. Brehm, A.M. Alleaume, J. Artelt, P. Bettencourt, E. Cassin, et al. 2005. Full-genome RNAi profiling of early embryogenesis in *Caenorhabditis elegans*. *Nature.* 434:462–469. <http://dx.doi.org/10.1038/nature03353>
- Stumpf, C.R., J. Kimble, and M. Wickens. 2008. A *Caenorhabditis elegans* PUF protein family with distinct RNA binding specificity. *RNA.* 14:1550–1557. <http://dx.doi.org/10.1261/rna.1095908>
- Tabach, Y., A.C. Billi, G.D. Hayes, M.A. Newman, O. Zuk, H. Gabel, R. Kamath, K. Yacoby, B. Chapman, S.M. Garcia, et al. 2013. Identification of small RNA pathway genes using patterns of phylogenetic conservation and divergence. *Nature.* 493:694–698. <http://dx.doi.org/10.1038/nature11779>
- Tatusov, R.L., N.D. Fedorova, J.D. Jackson, A.R. Jacobs, B. Kiryutin, E.V. Koonin, D.M. Krylov, R. Mazumder, S.L. Mekhedov, A.N. Nikolskaya, et al. 2003. The COG database: an updated version includes eukaryotes. *BMC Bioinformatics.* 4:41. <http://dx.doi.org/10.1186/1471-2105-4-41>
- Temme, C., M. Simonelig, and E. Wahle. 2014. Deadenylation of mRNA by the CCR4-NOT complex in *Drosophila*: molecular and developmental aspects. *Front. Genet.* 5:143. <http://dx.doi.org/10.3389/fgene.2014.00143>
- Timmons, L., D.L. Court, and A. Fire. 2001. Ingestion of bacterially expressed dsRNAs can produce specific and potent genetic interference in *Caenorhabditis elegans*. *Gene.* 263:103–112. [http://dx.doi.org/10.1016/S0378-1119\(00\)00579-5](http://dx.doi.org/10.1016/S0378-1119(00)00579-5)
- Toretsky, J.A., and P.E. Wright. 2014. Assemblages: functional units formed by cellular phase separation. *J. Cell Biol.* 206:579–588. <http://dx.doi.org/10.1083/jcb.201404124>
- Updike, D., and S. Strome. 2010. P granule assembly and function in *Caenorhabditis elegans* germ cells. *J. Androl.* 31:53–60. <http://dx.doi.org/10.2164/jandrol.109.008292>
- Updike, D.L., and S. Strome. 2009. A genomewide RNAi screen for genes that affect the stability, distribution and function of P granules in *Caenorhabditis elegans*. *Genetics.* 183:1397–1419. <http://dx.doi.org/10.1534/genetics.109.110171>
- Voronina, E., and G. Seydoux. 2010. The *C. elegans* homolog of nucleoporin Nup98 is required for the integrity and function of germline P granules. *Development.* 137:1441–1450. <http://dx.doi.org/10.1242/dev.047654>
- Weber, S.C., and C.P. Brangwynne. 2012. Getting RNA and protein in phase. *Cell.* 149:1188–1191. <http://dx.doi.org/10.1016/j.cell.2012.05.022>
- Wright, J.E., D. Gaidatzis, M. Senften, B.M. Farley, E. Westhof, S.P. Ryder, and R. Ciosk. 2011. A quantitative RNA code for mRNA target selection by the germline fate determinant GLD-1. *EMBO J.* 30:533–545. <http://dx.doi.org/10.1038/emboj.2010.334>
- Xue, B., R.L. Dunbrack, R.W. Williams, A.K. Dunker, and V.N. Uversky. 2010. PONDR-FIT: a meta-predictor of intrinsically disordered amino acids. *Biochim. Biophys. Acta.* 1804:996–1010. <http://dx.doi.org/10.1016/j.bbapap.2010.01.011>
- Yokoshi, M., Q. Li, M. Yamamoto, H. Okada, Y. Suzuki, and Y. Kawahara. 2014. Direct binding of Ataxin-2 to distinct elements in 3' UTRs promotes mRNA stability and protein expression. *Mol. Cell.* 55:186–198. <http://dx.doi.org/10.1016/j.molcel.2014.05.022>
- Zhang, Y., J. Ling, C. Yuan, R. Dubruielle, and P. Emery. 2013. A role for *Drosophila* ATX2 in activation of PER translation and circadian behavior. *Science.* 340:879–882. <http://dx.doi.org/10.1126/science.1234746>